Electronic Supplementary Material (ESI) for Catalysis Science & Technology.
This journal is © The Royal Society of Chemistry 2021
Please do not adjust margins

Electronic Supplementary Information

Copper (I) oxide nanoparticle-mediated C-C couplings for synthesis of polyphenylenediethynylenes: Evidence for homogeneous catalytic pathway

Fathima F. Pary[a§], Ravi Teja Addanki Tirumala[b§], Marimuthu Andiappan[b]*, Toby L. Nelson [a]*

[a.] *Department of Chemistry, Oklahoma State University, Stillwater, Oklahoma 74078, USA *Corresponding author Email ID: toby.nelson@okstate.edu*
[b.] *School of Chemical Engineering, Oklahoma State University, Stillwater, OK, USA *Corresponding author, Email: mari.andiappan@okstate.edu*
[§] These authors contributed equally

This file includes

Summary of Catalytic pathway of Cu_2O NPs-mediated oxidative C-C homocoupling of phenylacetylene

Figs. S1 to S9

Reference Cited for Electronic Supplementary Information

*Corresponding author, Email: mari.andiappan@okstate.edu

Please do not adjust margins

Please do not adjust margins

Summary of Catalytic pathway of Cu_2O NPs-mediated oxidative C-C homocoupling of phenylacetylene: The homocoupling of phenylacetylene (PA) was carried out at 110 ºC using spherical Cu_2O NPs with an average size of 34 nm (see Figure S2a). The samples of the reaction mixture were taken at frequent time intervals to quantify the reaction conversion using GC-MS analysis. The samples were also characterized using UV-Vis extinction spectra measurements to identify any possible formation of homogeneous copper (Cu) complexes. In Figure S1a, we show the PA conversion as a function of reaction time. As seen from Figure S1a, the complete conversion was observed in less than 9 hours under the reaction conditions investigated in this study. Diphenyldiacetylene (DPDA) was the only observed product during the reaction. In Figure S1b, we show the UV-Vis extinction spectra of reaction mixture measured before the addition of substrate (i.e., PA) and at different reaction times. As seen from Figure S1b, the extinction spectrum acquired before the addition of PA (i.e., t=0) shows only the extinction features of Cu_2O NPs. As the reaction starts after the addition of PA, new extinction peaks at ~385 and ~450 nm are evolved. We verified that the homocoupling product, DPDA, exhibits absorption peaks only in the 200-350 nm region. Therefore, the appearance of the new extinction peaks upon PA addition indicates the in-situ formation of homogeneous Cu complexes via PA-induced leaching of Cu_2O NPs surface atoms.

The presence of homogeneous Cu complexes, $[CuO(C_8H_5)_2]^-$ and $[CuO(C_8H_5)_2.H_2O]^-$, are confirmed using ESI-MS analysis of the supernatant solution of the reaction mixture as shown in Figure S1c. The ESI-MS analyzed the structure of the Cu complex, $[CuO(C_8H_5)_2]$, suggests that two PA (C_8H_6) molecules first adsorb on the surface of Cu_2O NPs (i.e., one molecule on surface Cu atom and another molecule on neighbouring surface O atom), and subsequently cause the leaching of Cu and O surface atoms. The second complex, $[CuO(C_8H_5)_2.H_2O]^-$, can then form from the first complex, $[CuO(C_8H_5)_2]^-$, and water (H_2O) molecule, which is the expected byproduct of oxidative C-C homocoupling of terminal alkynes. The leaching of Cu_2O NPs is also confirmed using TEM. Specifically, the size of Cu_2O NPs was reduced from the initial size of 34 ± 4 nm (see Figure S2a) to 16 ± 4 nm at the end of the reaction as shown in Figure S1d.

Two homogenous complexes, $[CuO(C_8H_5)_2]^-$ and $[CuO(C_8H_5)_2.H_2O]^-$, are observed in the ESI-MS spectra (Figure S1c). The density functional theory (DFT) calculations reported in our previous contributions confirm that these two complexes are expected to exhibit the UV-Vis extinction peak wavelengths of ~385 nm and ~450 nm, respectively.[1] Therefore, we assign the complexes observed at ~385 nm and ~450 nm in the UV-Vis extinction spectra (Figure S1b) to $[CuO(C_8H_5)_2]^-$ and $[CuO(C_8H_5)_2.H_2O]^-$, respectively. To illustrate the role of the homogeneous Cu complexes in the C-C homocoupling reaction, in Figure S1e, we plot the extinction intensity of Cu complex, $[CuO(C_8H_5)_2.H_2O]^-$ which shows UV-Vis extinction peak intensity ~450 nm, as a function of reaction time. Similar plot for the complex $[CuO(C_8H_5)_2]$- is shown in Figure S3a. It can be concluded from Figures S1c and S1e and Figure S3a that the concentration of homogenous Cu complexes changes with time and PA conversion as expected for the homogeneous catalytic species that participate in the catalytic cycle. It can also be observed in Figure S1e and Figure S3a that the concentrations of Cu catalytic species exhibit maxima followed by decreasing trend as the concentration of the reactant (i.e., PA) gets depleted with time. This trend is expected for the in-situ generated homogeneous catalytic species. Specifically, we attribute the decreasing trends in Figure S1e to the blackout or precipitation of homogeneous Cu catalytic species with the decreasing concentration of stabilizing species (i.e., PA). The presence of blacked-out Cu clusters (size = 4 ± 0.8 nm) is also confirmed at the end of the reaction sample as can be seen from the representative TEM image shown in Figure S1f. To further confirm that the observed homogenous Cu complexes are indeed catalytic species, we performed the reaction containing only the supernatant solution containing Cu complexes. The results from this experiment show that the Cu complexes are able to catalyze the homocoupling of phenylacetylene (PA) into complete conversion, as shown in Figure S3b.

 This journal is © The Royal Society of Chemistry 2020

Please do not adjust margins

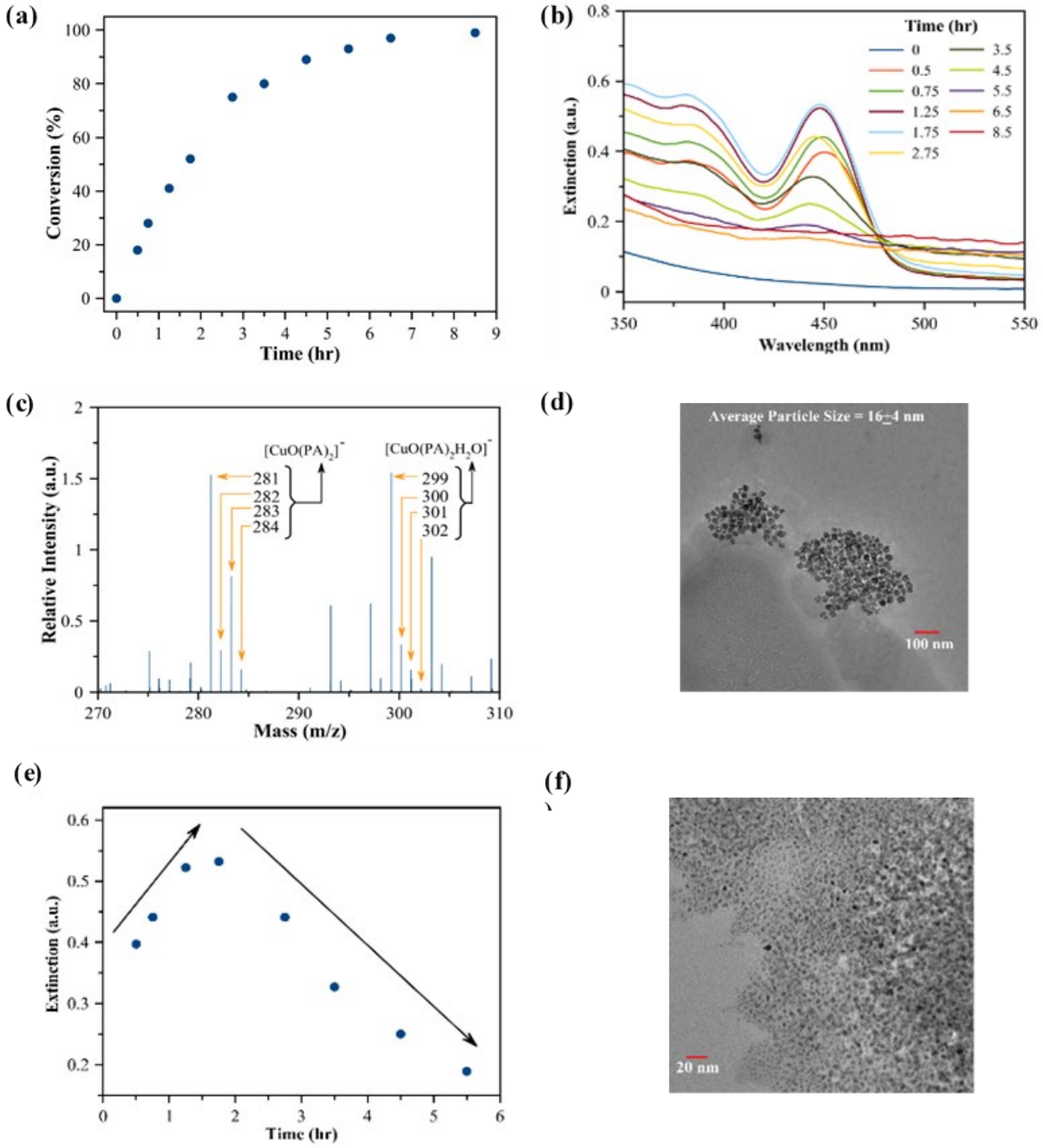

Fig. S1. (a) Conversion as a function of reaction time for the homocoupling reaction of PA at 110 ˚C. (b) UV-Vis extinction spectra of reaction mixture measured before the addition of PA (i.e., 0 % conversion) and at different reaction conversions during the homocoupling reaction of PA at 110˚C. (c) Representative ESI-MS spectra of $[CuO(C_8H_5)_2]^-$ and $[CuO(C_8H_5)_2H_2O]^-$. (d) Representative TEM image of Cu_2O nanoparticles observed in the reaction mixture at the end of the reaction (Average size of Cu_2O NPs = 16 ± 4 nm). (e) Extinction intensity at the peak wavelength of ~450 nm in the UV-Vis extinction spectrum of the reaction mixture as a function of reaction time. (f) Representative TEM image of blacked-out nanoclusters observed in the reaction solution at the end of the reaction (Average size of nanoclusters = 4 ± 0.89 nm).

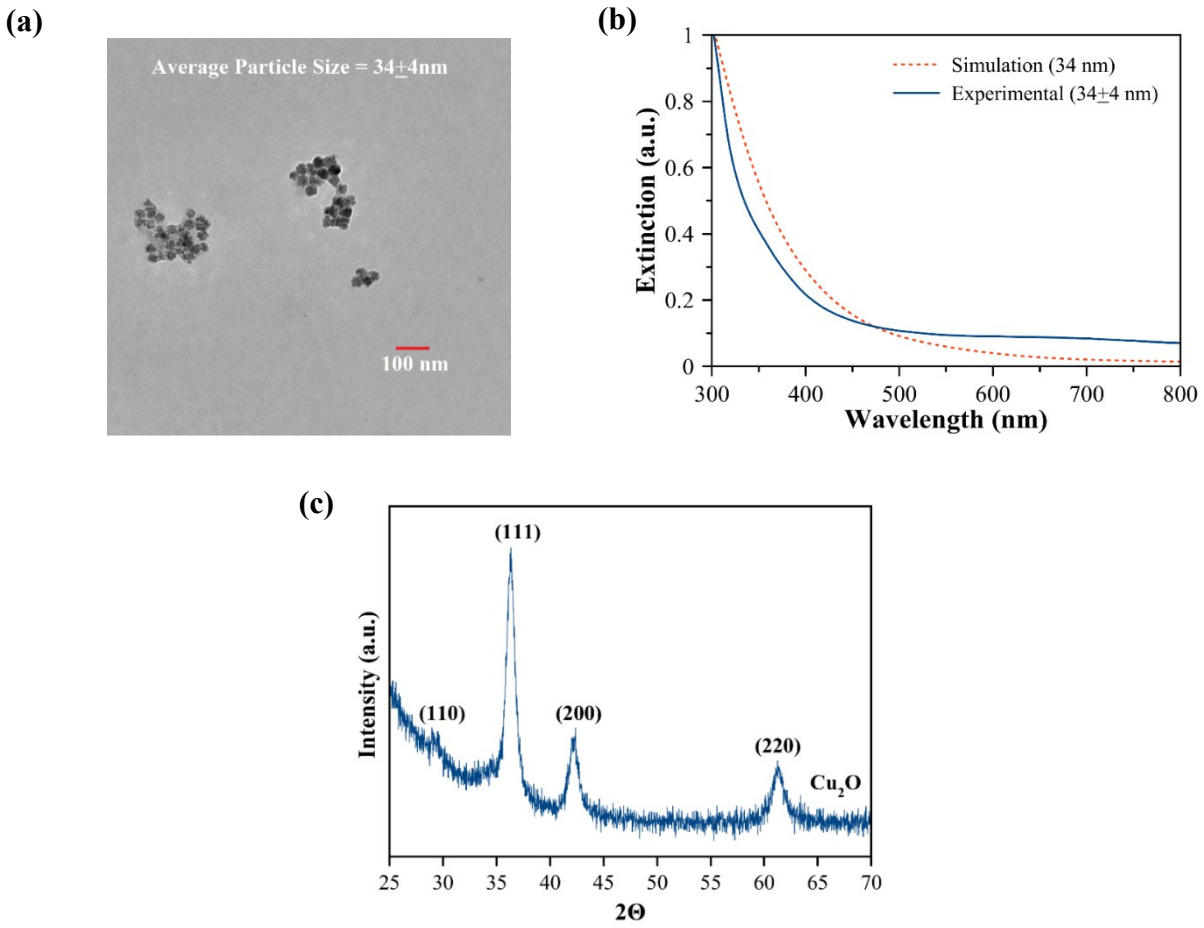

Fig. S2. (a) A representative TEM image of the Cu_2O nanoparticles (34±4 nm). (b) Comparison of experimental and computational measurement of UV-Vis extinction spectrum for Cu_2O nanoparticles for the particle size 34 nm. (c) The X-ray diffraction pattern of the Cu_2O nanoparticles.

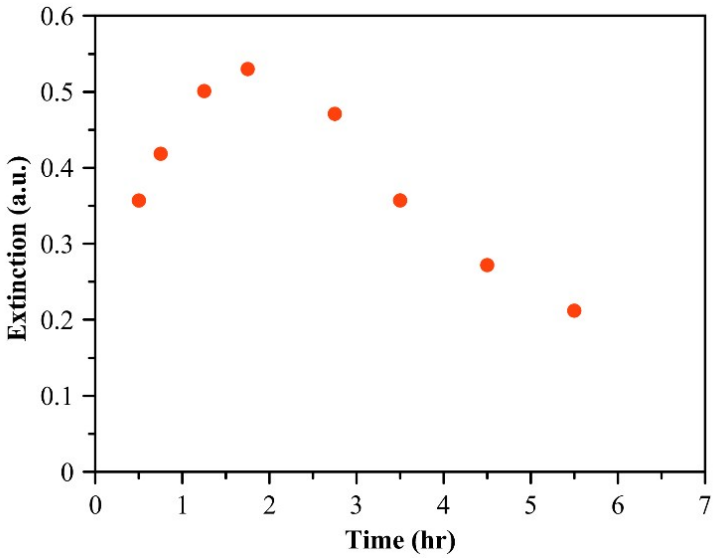

Fig. S3a. Extinction intensity at the peak wavelength of ~385 nm in the UV-Vis extinction spectrum of the reaction mixture as a function of reaction time.

This journal is © The Royal Society of Chemistry 2020

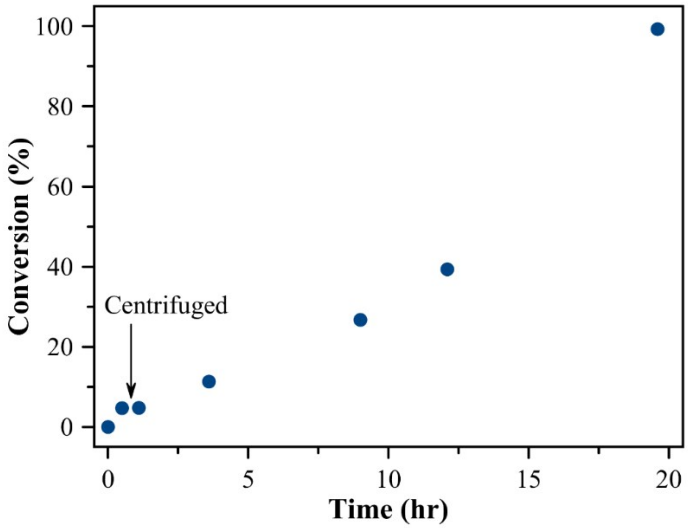

Fig. S3b. Conversion as a function of reaction time for homocoupling of PA at 110 ˚C, where the gas used was dry air. After the end of 30 minutes into the reaction, it was stopped and Cu_2O nanoparticles were removed from the reaction mixture using centrifugation. The reaction is continued under same conditions using Cu complexes in supernatant solution as the solitary catalyst.

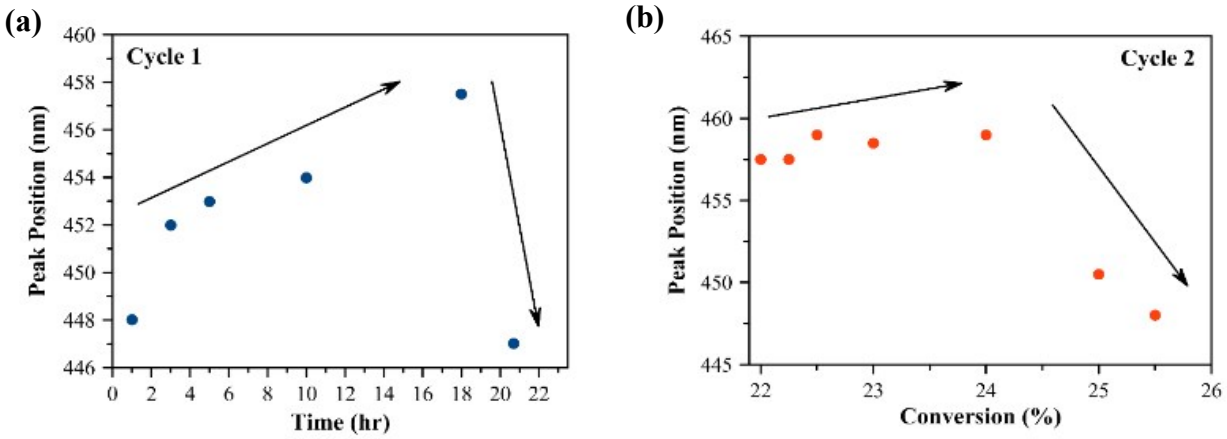

Fig. S4. (a) Peak position for OHR of PA at 110 ˚C in the presence of base, where the gas was switched from N_2 to Dry Air after 20 h of reaction time for Cycle 1. (b) Peak position for OHR of PA at 110 ˚C in the presence of base, where the gas was continued to be Dry Air after end of first cycle, for Cycle 2.

Please do not adjust margins

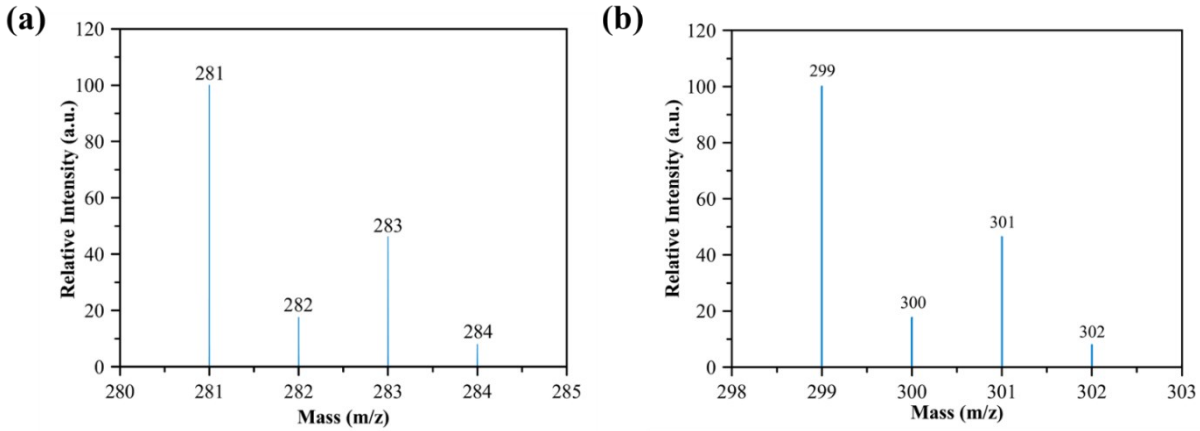

Fig. S5. (a) Predicted mass spectrum for the proposed copper complex with chemical formula, $[CuO(PA)_2]$-. (b) Predicted mass spectrum for the proposed copper complex with chemical formula, $[CuO(C_8H_5)_2.H_2O]$-.[2]

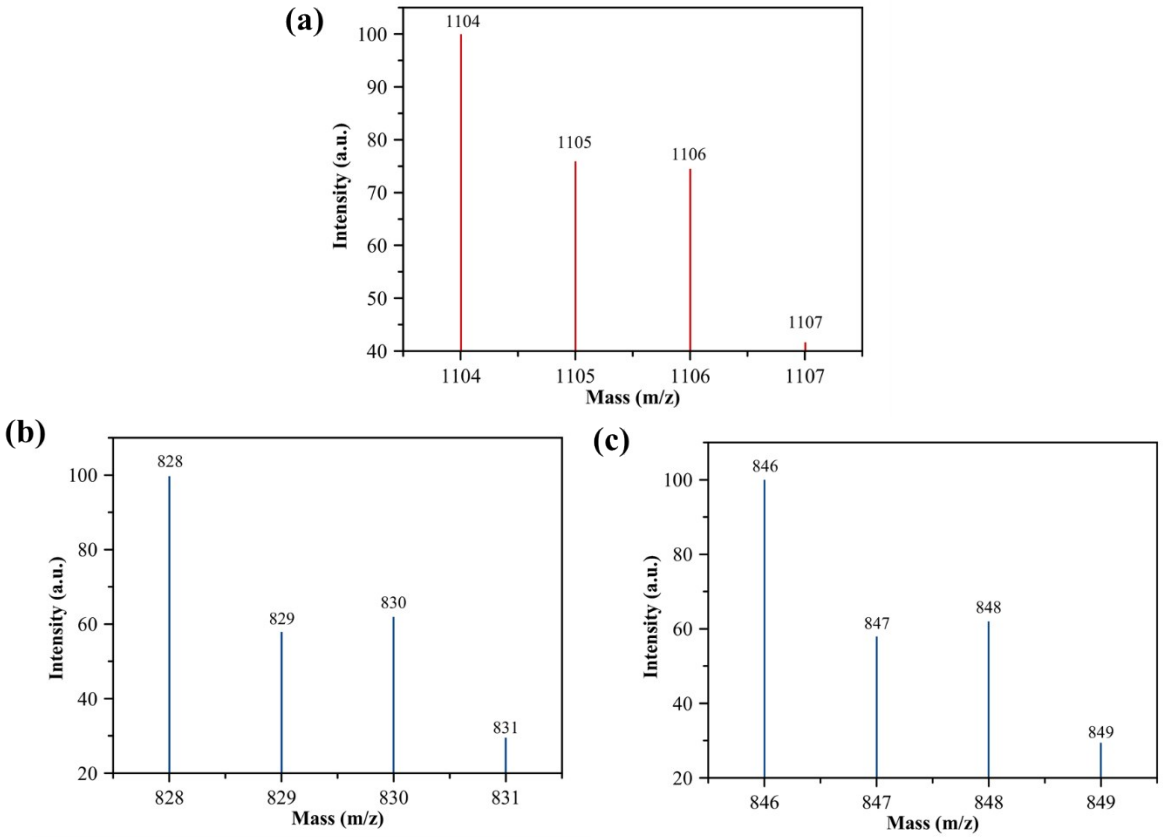

Fig. S6. (a-c) Predicted mass spectra for the proposed copper complex with chemical formula $[CuO(C_{68}H_{106}O_4).2H_2O)]^-$, $[Cu(C_{52}H_{74}O_4)]^-$, $[Cu(C_{52}H_{74}O_4\ H_2O)]^-$ that match with the experimentally measured ESI-MS spectra shown in Figure 3a, 3b and 3c, respectively, in the main draft.[2]

This journal is © The Royal Society of Chemistry 2020

Please do not adjust margins

1H NMR of 1,4-bis(dodecyloxy)-2,5-diethynylbenzene.

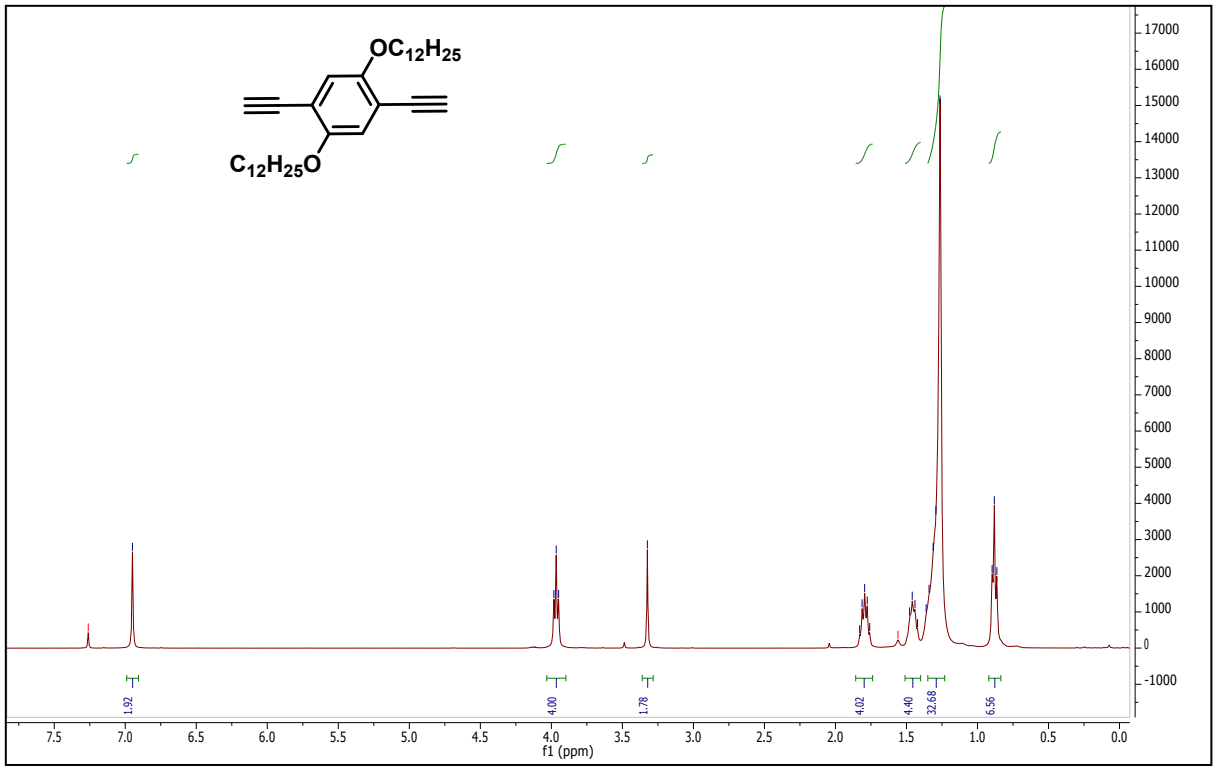

^{1}H NMR of 1,4-bis((2-ethylhexyl)oxy)-2,5-diethynylbenzene.

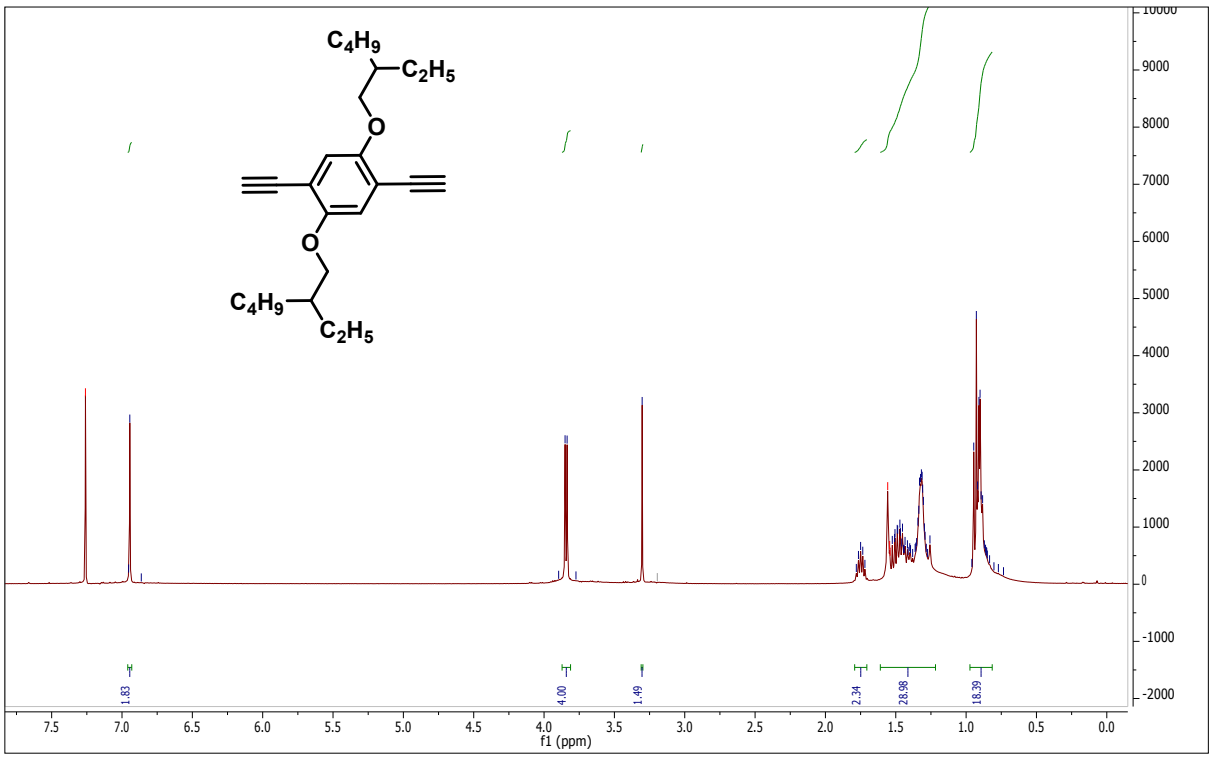

^{1}H NMR of poly (1,4-bis(dodecyloxy)-2,5-diethynylbenzene).

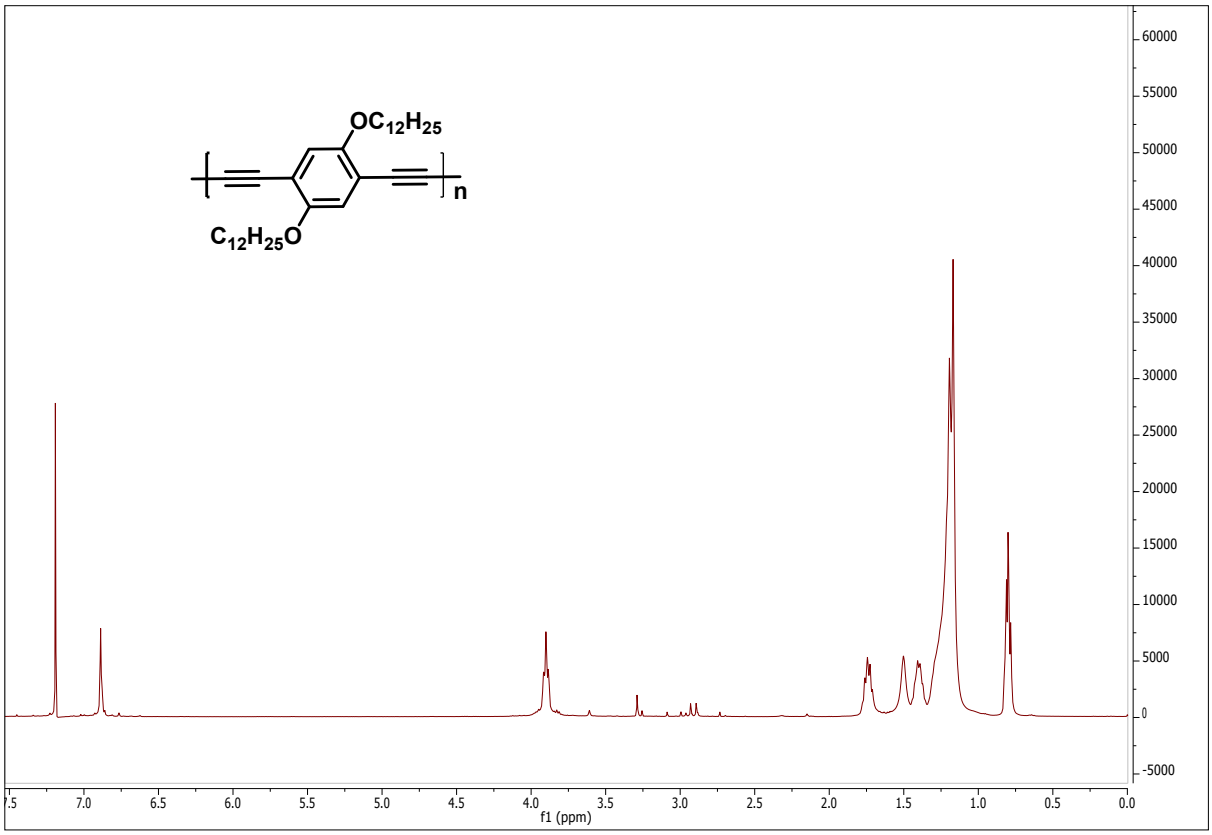

^{1}H NMR of poly(1,4-bis((2-ethylhexyl)oxy)-2,5-diethynylbenzene)

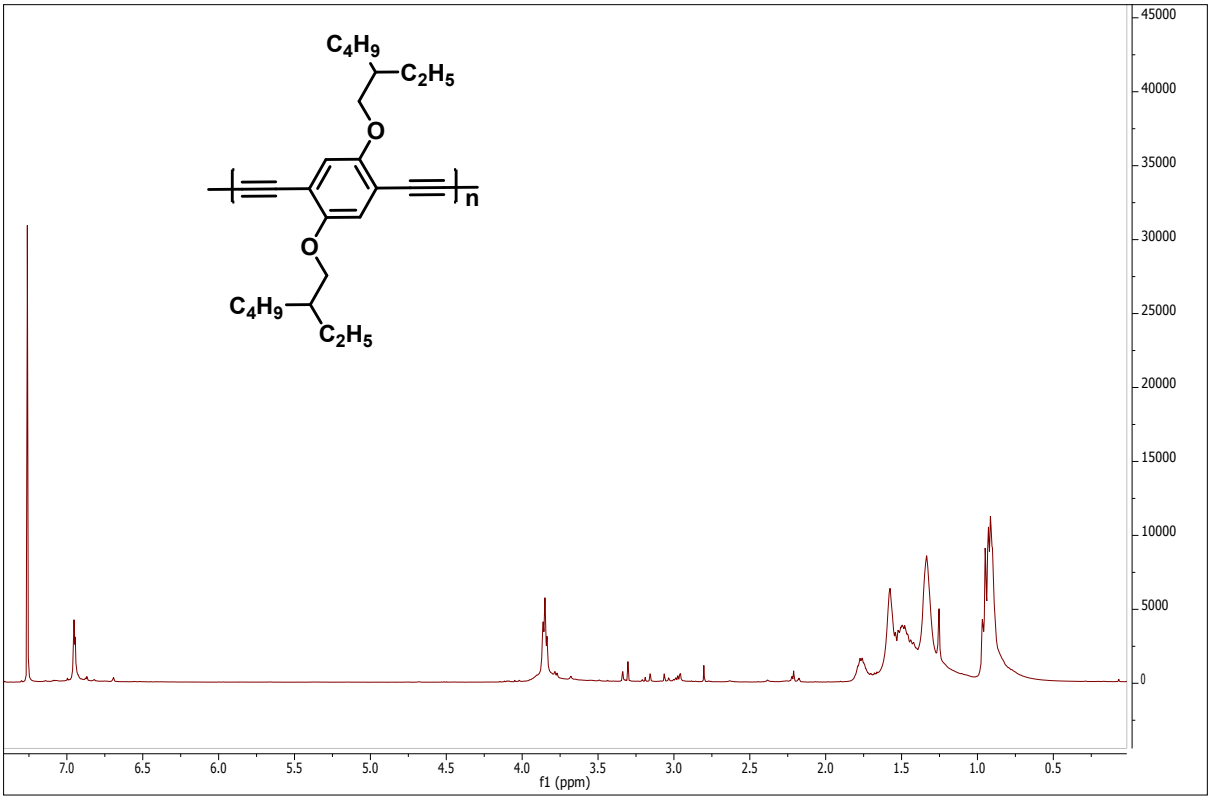

This journal is © The Royal Society of Chemistry 2020

Please do not adjust margins

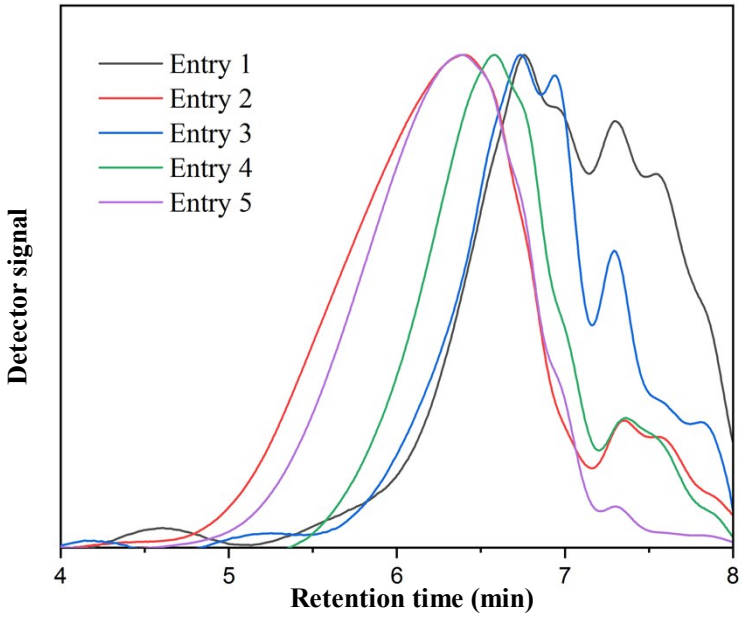

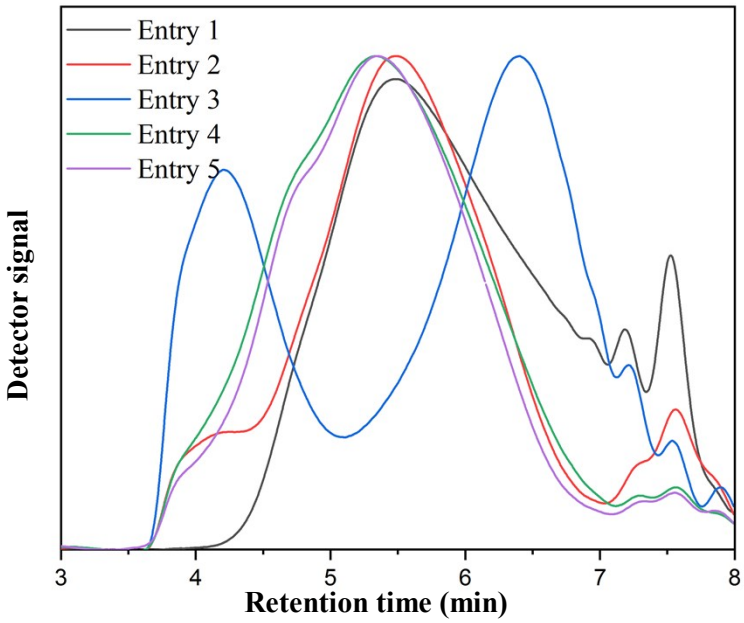

Fig. S7. GPC traces of synthesized polymers of **1a** discussed in Table 1.

Fig. S8. GPC traces of synthesized polymers of **1b** discussed in Table 2.

Reference Cited for Electronic Supplementary Information

1 R. T. Addanki Tirumala, A. P. Dadgar, F. Mohammadparast, S. B. Ramakrishnan, T. Mou, B. Wang and M. Andiappan, *Green Chem.*, 2019, **21**, 5284–5290.

2 Isotope Distribution Calculator, Mass Spec Plotter, Isotope Abundance Graphs, https://www.sisweb.com/mstools/isotope.htm, (accessed December 20, 2019).

This journal is © The Royal Society of Chemistry 2020

Please do not adjust margins

Please do not adjust margins

This journal is © The Royal Society of Chemistry 2020

Please do not adjust margins